17

The Development of Novel *In Vitro* Binding Assays to Further Elucidate the Role of tRNAs in Protein Synthesis

Anthony J. Bell, Jr.*, Suzanna Ellzey, Devin McDougald and Crystal Serrano
Department of Chemistry and Biochemistry, The University of Southern Mississippi, USA

1. Introduction

The accurate translation of the genetic information encoded by mRNA into proteins is critical for proper cellular function. Transfer ribonucleic acids (tRNAs) are essential biomolecular linkers that help maintain translational fidelity by accurately connecting genotype (mRNA) to phenotype (protein) during protein synthesis. The initial stages of ribosomal protein synthesis are controlled by aminoacyl-tRNA synthetases (AARSs). AARSs initiate protein synthesis by catalyzing the acylation of tRNAs to their cognate amino acids. The resulting aminoacyl-tRNAs (aa-tRNAs) are transported to the ribosome by the translation factor Elongation Factor (EF-Tu) to undergo peptide bond formation. The synergistic interplay among the protein translational machinery involved in this process is highly regulated and extremely accurate. In *E. coli*, the error rate for protein synthesis correlates to roughly 1 misincorporation per 10^4 codons translated (Husaain et al., 2006; Loftield & Vanderjagt, 1972; Ogle & Ramakrishnan, 2005; Rosenberger & Foskett, 1981; Roy & Ibba, 2006). The high level of stringency is the result of substrate discrimination that can occur at four different translation checkpoints: 1) amino acid activation, 2) aminoacylation, 3) aa-tRNA transport to the ribosome (via EF-Tu) and 4) initial binding of aa-tRNAs within the ribosome. The molecular recognition events mediated by AARSs in checkpoints 1 and 2 provide the highest level of stringency. *In vitro* studies have shown that AARSs possess a discrimination factor of 200 – 10,000 during amino acid activation; the stringency factor increases to > 10,000 during aminoacylation (Giege et al., 1998; Ling et al., 2009; Reynolds et al., 2010). EF-Tu binding interactions provide an additional, albeit lower, degree of stringency in step 3. Reports show that EF-Tu binds cognate aa-tRNAs with nearly identical affinities, while noncognate or misaclyated aa-tRNAs possess extremely broad EF-Tu binding affinity profiles (~ 700-fold difference between noncognate aa-tRNAs) (Dale & Uhlenbeck; 2005). It is presumed that these species are removed from the translation pathway by EF-Tu to further enhance fidelity. Despite the large amount of studies focused on defining the intricacies of translation, there are still a number of unanswered questions regarding the basic tenants of translation. Two intriguing questions are: *i) do tRNAs play an active or passive role in the regulation of translation and ii) why is ribosomal protein synthesis limited to 20 amino acids?* An interrelated question that we would like to address is: *can in vitro binding assays be used to accurately define the mechanisms of cellular protein synthesis?* This chapter focuses on current and the development of two *in vitro* binding assays that are designed to investigate the role of tRNA in the initial and intermediate stages of translation. The new assays offer rapid, sensitive and straightforward techniques to monitor the role of tRNA in: activation,

aminoacylation and aminoacyl transport. A more detailed view of the role of tRNA in ribosomal protein synthesis could provide invaluable insight into the evolutionary role of tRNA in protein synthesis. Moreover, this information could prove essential in the development/ adaptation of *in vitro* bacterial translation systems to synthesize novel biomolecules (i.e. peptidomimetics).

2. The adaptor hypothesis

The characterization of tRNA has been a focal point of chemical biology since first postulated by Francis Crick in the Adaptor hypothesis in the late 1950s (Crick, 1958). According to Crick, accurate protein synthesis required: i) a nucleic acid template, ii) an adaptor molecule that carried an amino acid to the template and iii) an organized binding arrangement between the template and the adaptor. Research would later reveal the template as mRNA and the adaptor as tRNA – while the organized binding interactions correlate to hydrogen-bonds between the codon and the anticodon of each species. Crick's hypothesis went further to accurately predict the existence (and editing capability) of AARSs. Although certain aspects of the Adaptor Hypothesis related to AARS functionality were disproven (i.e. a single AARS is not solely dedicated to the aminoacylation of an individual tRNA) (Martin et al., 1977; Wilcox & Nirenber, 1968; White & Bayley, 1972) the ideas put forth by Crick helped enable a more accurate conceptualization protein synthesis. The Adaptor Hypothesis also laid the groundwork for establishing and ultimately deciphering the genetic code.

2.1 Protein translation

tRNAs enter the protein synthesis pathway during the second stage of protein synthesis (Figure 1). tRNAs are acylated or "charged" with amino acids by AARSs and the resulting aa-tRNAs are transported to the ribosome by EF-Tu (step 3). The final stages of protein translation are initiated in step 4 as each aa-tRNA undergoes initial binding to mRNA within the A-site of the ribosomal 50S large subunit. The remaining translation factors EF-Ts and EF-G are responsible for the reactivation of EF-Tu and movement (or translocation) of each aa-tRNA along the mRNA template. Finally, ribosomal release factors (RFs1–3 and RRF) mediate the termination and release of the protein from the ribosome. After completing one round of synthesis, the translational machinery (i.e. tRNAs, AARSs and translation factors) is free to re-enter the synthesis pathway to generate new proteins. Each translational component is critical but tRNA is extremely important because it is involved in nearly *every* stage of protein synthesis.

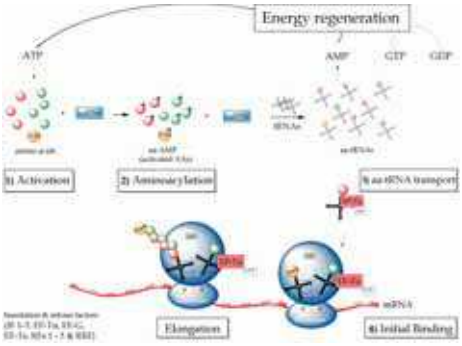

Fig. 1. Schematic of *E. coli* ribosomal protein synthesis.

2.1.1 Characterization of transfer ribonucleic acids (tRNAs)

Zamecnick and Hoagland achieved one of the first major breakthroughs toward the discovery of tRNA in 1957. Their work showed that a radiolabelled amino acid becomes covalently attached to a "soluble RNA" species (later reclassified as tRNA) when incubated with ATP and cellular extracts (Hoagland et al., 1957). In the following year Zachau et al., demonstrated that an ester bond (between a nucleic acid 3' adenine and ^{14}C-Lue) provided the attachment site (Zachau et al., 1958). Robert Holley and his colleagues reached another major milestone in 1965 by successfully determining the complete sequence of tRNA^{Ala} from yeast (Holley et al., 1965). These achievements helped confirm the existence of tRNA as the adaptor molecule proposed by Crick and have ushered in a series of discoveries devoted to the characterization of tRNAs.

2.1.2 Structural features of tRNAs

tRNAs may be most well known for their cloverleaf-like shape. Figure 2a displays the cloverleaf structure embedded within a precursor tRNA. Prior to translation, *E. coli* precursor tRNAs undergo enzymatic cleavage reactions at their 5' and 3' ends. 5'-end processing is carried out by the endonuclease RNase P (Frank & Pace, 1998), while 3'processing is mediated by a variety of endo- and exonucleases (Morl & Marchfelder, 2001). The exact sequence of events and identity of the nucleases involved in 3' processing are still undetermined. Once fully processed, the resulting tRNA is composed of the five canonical structural regions labelled in Figure 2b; clockwise from the 3' end is the: acceptor stem, T-arm, variable loop, anti-codon loop and D-arm.

The acceptor stem and the anticodon loop are arguably, the most well known of the five structural regions (Figure 2b). The acceptor stem encompasses both ends of the molecule, including the -CCA terminal sequence. The –CCA sequence is encoded in all *E. coli* tRNAs genes and serves as the site of attachment for amino acids. Aminoacylation does not occur if the integrity of the –CCA terminal sequence is not intact. In the event of mutations or damage to the 3' end, the tRNA maturation/ repair enzyme tRNA nucleotidyltransferase (TNT) is upregulated. In eukaryotes, TNT is responsible for 3' end maturation by accurately synthesizing the final three nucleotides (–CCA) in a template independent fashion (Deutscher, 1982; Sprinzl & Cramer, 1979; Yue et al., 1996). TNT carries out a similar task in *E. coli* if the –CCA end is altered (Zhu & Deutscher, 1987). The anticodon loop is located on the opposite end of the molecule. The anticodon loop is composed of 7 nucleotides, including the anticodon triplet. The first nucleotide of the anticodon can deviate from Watson-Crick hydrogen-bond patterns. This phenomenon known as "wobble" facilitates the degeneracy of the genetic code by permitting mRNA codons to bind multiple tRNA anticodons.

The identity and composition of tRNA bases are also very intriguing. tRNAs contain a number of highly conserved bases within the arms (T- and D-) and the anticodon loop (labelled white in Figure 2c). Conserved bases serve a variety of functions ranging from maintaining structural integrity to providing favourable contact sites for AARSs and EF-Tu during aminoacylation and aa-tRNA transport. A number of tRNA bases also possess additional or nonstandard functional groups (i.e. thiol and methyl groups). This class of nucleotides is referred to as "hyper-modified". To date > 100 tRNA hyper-modified bases have been characterized, with some such as pseudouridine possessing strong evolutionary conservation (Dunin-Horkawicz et al., 2006; Iwata-Reuyl, 2008; Rozenski et al., 1999). These structural and chemical characteristics indicate that tRNAs are highly conserved biomolecules that are equipped with an appreciable amount of chemical diversity.

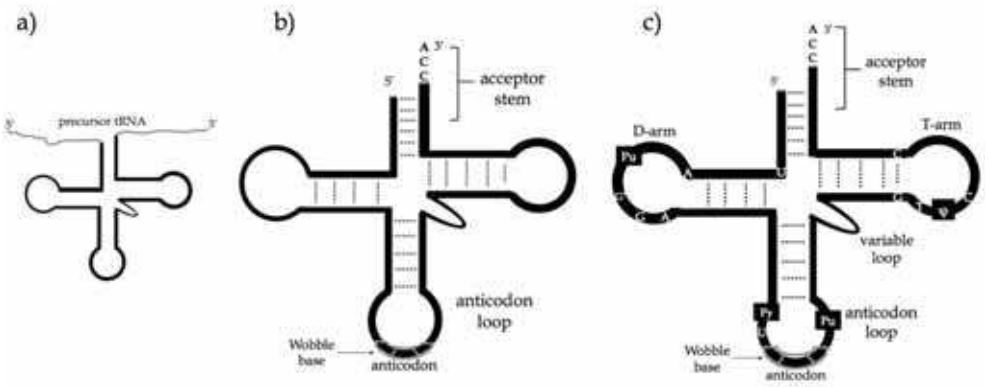

Fig. 2. tRNA structures before and after 5' and 3' end processing. Panel a) displays precursor tRNA. Panel b) displays the acceptor stem and anticodon loop regions. Panel c) displays the five canonical tRNA secondary structural elements including the T-arm, variable loop and D-arm. Bases indicated in panel c): A = adenosine, G = guanine, C = cytosine, U = uracil, Pu = purine, Py = pyrimidine and ψ = pseudouridine.

2.1.3 Aminoacylation of tRNAs

Aminoacylation is initiated by AARSs. AARSs are highly specific enzymes that bind their cognate amino acid in the presence of ATP and transfer the innermost phosphate from ATP to the amino acid. This process is referred to as "activation" because the resulting adenylate species, AA-AMP, is highly energetic. AA-AMPs remains tightly associated with their AARS until the AARS•AA-AMP complex encounters a tRNA molecule. At this stage translational fidelity is based on the interplay between the AARS and the tRNA, in that only cognate (correct) tRNAs are acylated at a much higher level than noncognate tRNAs. Figure 3 displays a schematic of activation (step *i*) and aminoacylation (step *ii*).

$$\text{AA} + \text{ATP} + \text{AARS} \rightleftharpoons \text{AARS•AA-AMP} + \text{PPi} \qquad (i)$$

$$\text{AARS•AA-AMP} + \text{tRNA} \rightleftharpoons \text{AARS} + \text{aa-tRNA} + \text{AMP} \qquad (ii)$$

Fig. 3. Schematic of the translational machinery that mediate the early stages of ribosomal protein synthesis: step *i*) amino acid activation and step *ii*) aminoacylation.

A more detailed view of each reaction is shown in Figure 4. During activation, the AARS binds the amino acid and orients the α-carboxylate of the amino acid toward the α-phosphate of ATP. This alignment promotes an in-line nucleophilic displacement reaction as shown in panel a. The resulting adenylate (AA-AMP) remains bound to the AARS until it encounters a tRNA molecule (panel b). The incoming tRNA binds the AARS, which subsequently aligns the AA-AMP and tRNA. Next, the 2' or 3' hydroxyl of the tRNA initiates acylation via nucleophilic attack on the α-carboxylate of the amino acid adenylate as shown in panel c. Finally, the aa-tRNA is generated, AMP is released and the AARS is free to catalyze new activation and aminoacylation reactions.

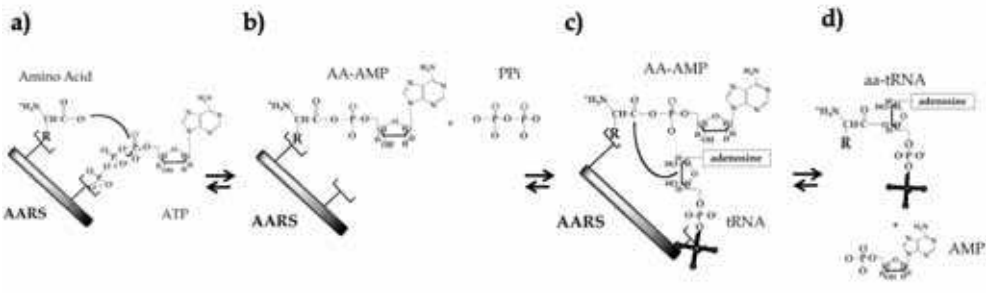

Fig. 4. Graphical representation of activation (b) and aminoacylation (d).

3. Importance of *in vitro* tRNA aminoacylation assays

Activation and aminoacylation are closely linked; in fact these steps are often depicted as a single reaction. Although both reactions occur at a rapid rate, it is important to understand the mechanistic details of both separately in order to determine the influence that each has on translational fidelity. The section of this chapter will focus on the latter, aminoacylation. *In vitro* aminoacylation assays are advantageous because this reaction format enables the user to measure both the rate and the level of aminoacylation. While *in vivo* assays, despite being the physiological benchmark for translation, only provide data that reflects the level of aminoacylation. Despite a large amount of research using both assay formats, there are several examples of conflicting results between *in vitro* and *in vivo* experiments. It is not surprising that *in vivo* and *in vitro* data generate conflicting results since proteins are the product of a biological paradox. In that, native proteins (i.e. full-length proteins without mutations or truncations etc.) possess an enormous level of accuracy despite being manufactured over a short period of time. Developing *in vitro* and *in vivo* assays that accurately define how the two seemingly opposing forces of: *translational speed* and *translational accuracy* coexist is a very complicated task. This point is more clearly shown by the discrepancies that exist between *in vivo* and *in vitro* experiments designed to determine the effect that the G3•U70 $tRNA^{Ala}$ recognition element on aminoacylation. *In vitro* assays showed that mutations within the recognition element drastically reduced aminoacylation (Beuning et al, 1997; Frankyln & Schimmel, 1989; Hou & Schimmel, 1988; McClain et al., 1988; Musier-Forsyth et al., 1991). While *in vivo* experiments indicated that mutations within the recognition element had a minimal effect (Gabriel et al., 1996; McClain et al., 1999). Despite advancements in *in vitro* and *in vivo* assays, a number of discrepancies between the two formats remain. This section will focus on current and new assays designed to provide a more clear view of aminoacyaltion.

3.1 *In vitro* aminoacylation assays using radioactive amino acids

The most predominately used *in vitro* aminoacylation assay is based on the techniques developed by Zamecnick et al. using ^{14}C labelled amino acids (Hoagland et al, 1957). The assay measures the rate of formation of radiolabelled aa-tRNAs under steady state conditions. The reaction is initiated by titrating a labelled amino acid into a reaction vessel containing the cognate AARS, tRNA and ATP (complete buffer composition detailed in Figure 6).

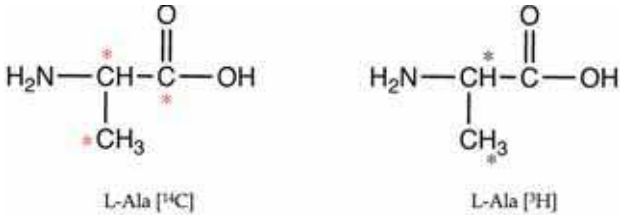

Fig. 5. Schematic of L-alanine illustrating the potential isotopic labelling sites for ^{14}C (red) and ^{3}H (grey).

Aminoacylation is recorded by: *i)* removing aliquots at different time points, *ii)* spotting each aliquot onto pre-soaked nitrocellulose filters [soaked with tricholoroacetic acid (TCA)], *iii)* washing each filter with excess TCA and 95% ethanol. Finally, each filter is dried and placed into a scintillation vial. The amount of ^{14}C or ^{3}H precipitated onto the filter is recorded using a scintillation counter. The major steps of this reaction are displayed below in Figure 6.

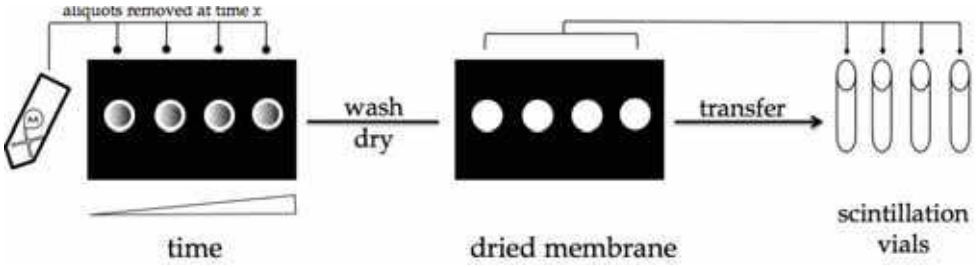

Fig. 6. Diagram of common method to measure aminoacylation using radioactive amino acid substrates. Reaction buffer: 50 mM HEPES (or Tris-HCl) pH 7.5, 2 mM ATP, 10 mM $MgCl_2$, 4 mM DTT, 20 mM KCl, bovine serum albumin (0.2 mg/ mL). Nitrocellulose membranes pre-soaked in excess TCA to ensure the maximum level of precipitation.

The level of aminoacylation is determined indirectly by first calculating the amount radiolabelled amino acid that is bound to a filter (at time *x*) (Eigner & Loftield, 1974; Loftield, 1974). The amount of precipitated amino acid is determined from the specific activity of the amino acid and the scintillation counting efficiency. The level of aminoacylation is determined by dividing the amount of labelled aminoacyl tRNA (bound to the filter) by the total input tRNA. Although this assay is widely used, there are significant drawbacks associated with it. One major limitation is related to the indirect nature of the readout. The assay does not stringently distinguish active (acylated) from inactive (non-acylated) tRNAs. This is a large potential source of error that could lead to incorrect aminoacylation values. Other limitations are related to the use of ^{14}C and ^{3}H labelled amino acids. Radiolabelled amino acids are generally limited to the 20 L-amino acids. Hence, the analysis of unnatural (non-L) amino acids is prohibited. Also large amounts of substrate are required due to the low affinity AARS have toward their cognate amino acid (K_M values range of μM to mM) (Eriani et al., 1993; Hill & Schimmel, 1989; Ibba et al., 1996). To offset the accompanying high levels of radioactivity, extremely high amounts of tRNA must be supplied or the concentration of the amino acid must be reduced

to levels that are below saturating conditions. The latter set of conditions (i.e. reducing amino acid concentrations) prohibits the use of this assay to monitor pre-steady state kinetics because the specific activity of each radioisotope is too low to generate a reliable signal. Based on these issues, there is clearly a need to develop alternate methods to measure aminoacylation.

3.2 *In vitro* aminoacylation assays using radioactive tRNAs

3.2.1 Aminoacylation of nicked ^{32}P labelled tRNAs

One technique that has emerged as an alternative to the radiolabelled amino acid assay is based upon on using ^{32}P-labeled tRNAs. This approach, pioneered by the Uhlenbeck laboratory offers a number of advantages vs. the classical aminoacylation assay. Their initial strategy employed ^{32}P-labeled "nicked" tRNAs as substrates (Wolfson et al, 1998). The tRNA was prepared by annealing a longer unlabelled ribonucleic strand to a shorter ^{32}P-labeled strand. The longer strand (57-nt) encompassed the majority of the tRNA (5' acceptor region, D-arm, anticodon, variable loop and part of the T-arm); while the shorter strand (19-nt) encompassed a portion of the T-arm and acceptor stem. The longer strand was generated via *in vitro* transcription using T7 RNA polymerase. The shorter strand was generated via standard chemical synthesis and subsequently labelled with ^{32}P-γ-ATP using T4 polynucleotide kinase (T4PNK). A schematic of the resulting tRNA is shown in Figure 7b, the position of the radiolabel within the T-arm is denoted with an arrow.

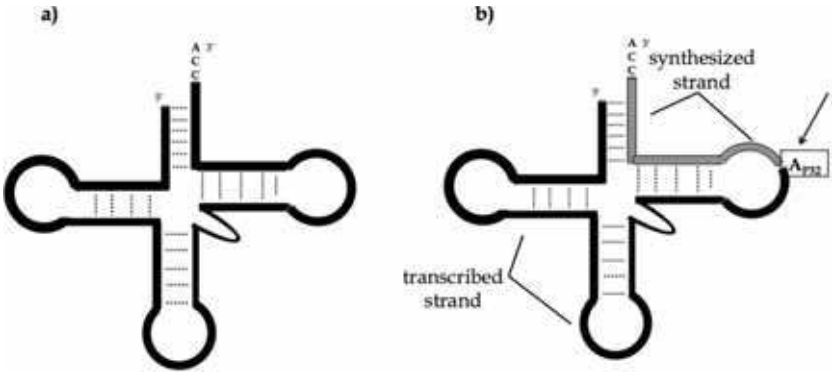

Fig. 7. Schematic of intact (a) vs. nicked (b) tRNAs. The *in vitro* transcribed strand is shown in black and the chemically synthesized strand is shown in grey.

To initiate the assay, radiolabelled tRNA is incubated with an amino acid and AARS of interest. The reaction is then quenched and loaded onto an acid denaturing polyacrylamide gel. Since aa-tRNAs possess a relatively larger positive charge than non-acylated tRNAs, aa-tRNAs migrate slower than the non-acylated tRNAs. The level of aminoacylation is measured by dividing the number of counts of the aminoacylated tRNA by the number of counts of non-acylated tRNA (counts measured via Phosphorimager analysis). The ability to distinguish aa-tRNAs from nonacylated tRNAs in a straightforward manner significantly reduces the level of error associated with this assay *vs.* the assay using radiolabelled amino acids. The ^{32}P isotope also provides a much stronger signal than ^{14}C and ^{3}H, this feature permits the use of much lower amounts of

amino acid. As a result, this assay is capable of measuring aminoacylation at pre- and steady state conditions. The expense and variable stability of ^{14}C or ^{3}H amino acids also add to the attractiveness of an alternate assay. Finally, the use of ^{32}P labelled tRNAs provides a method to measure the aminoacylation of unnatural amino acids. Despite its advantages, the nicked tRNA assay has drawbacks related to safety, compatibility and run time. The high-energy ^{32}P isotope requires the use of protective shielding and typical run times range from 12-16 h to fully separate the acylated and non-acylated tRNAs. Taken as a whole the benefits of this assay outweigh the disadvantages, but there is still room for improvement.

3.2.2 Aminoacylation of full-length ^{32}P labelled tRNAs

Uhlenbeck et al. improved the nicked tRNA assay by making several key adjustments (Wolfson & Uhlenbeck, 2002). The first was related to the positioning of the ^{32}P radiolabel. The repair/ processing enzyme terminal nucleotidyl transferase (TNT) was used to label the 3'-end of the tRNA. TNT labels tRNAs by exchanging the 3'-terminal non-labelled ("cold") adenosine with a ^{32}P-α-adenosine to yield a new 3' radiolabelled tRNA. This step is displayed in Figure 8a; the radiolabelled product is denoted in red. This labelling procedure circumvents the two-step process associated with the preparation of nicked tRNAs. The aminoacylation reaction is identical to the approach described in section 3.2.1. The next major change involves the use of nuclease P1 or S1 to separate aminoacylated from non-acylated tRNAs. Both endonucleases digest aa-tRNAs to yield two products: ^{32}P-AA-AMP and 5' monophosphates. aa-tRNAs represent the former and nonacylated tRNAs the latter. Each radioactive species is separated clearly and rapidly via thin layer chromatography (TLC). This step obviates the lengthy run times associated with acid gel electrophoresis. The level of aminoacylation is recorded by dividing the number of counts of the ^{32}P-AA-AMP species by the counts of 5' monophosphates (^{32}P-AMP). Figure 8 displays a schematic of the labelling (step a) and hydrolysis of 3'-^{32}P-aa-tRNAs.

Due to the sensitivity of the ^{32}P isotope, this assay can measure the rate of aminoacylation at pre- and steady state conditions. As stated earlier, pre-steady state analysis is essentially not feasible with the conventional aminoacylation assay.

The ^{32}P tRNA assay also provides enhanced user flexibility. As a result, the steady state reaction conditions can be altered to more closely resemble *in vivo* conditions. Wolfson & Uhlenbeck exploited this feature to investigate the discrepancies between *in vitro* and *in vivo* assays, describing the role of the G3•U70 $tRNA^{Ala}$ recognition element (Wolfson & Uhlenbeck, 2002). As discussed in section 3, *in vitro* assays indicated that changes within the recognition element significantly reduced the rate of aminoacylation, while *in vivo* experiments showed that mutations within the recognition element produced a minimal effect. Since the reaction conditions of the ^{32}P assay are more amenable to alerations, the amounts of inorganic pyrophosphatase (PiPase) and EF-Tu were increased to levels that more closely resemble *in vivo* conditions. The level and rate of aminoacylation were shown to be clearly dependent upon the reaction conditions. Under standard *in vitro* conditions (i.e. reduced levels of PiPase and in the absence of EF-Tu), the rate and the level of aminoacylation was strongly affected by the integrity of the G3•U70 $tRNA^{Ala}$ recognition element. Mutations within the recognition element showed a significant reduction in the both the rate (reduced k_{cat}/K_M) and the level of aminoacylation. Upon

increasing the concentration of PiPase and EF-Tu to near *in vivo* levels, the level of aminoacylation showed the opposite effect (a marked increase in aminoacylation). These results clearly show the power of this assay. As a result, the intricacies of aminoacylation can be investigated over a wider range of conditions that conventional *in vitro* and *in vivo* assays cannot.

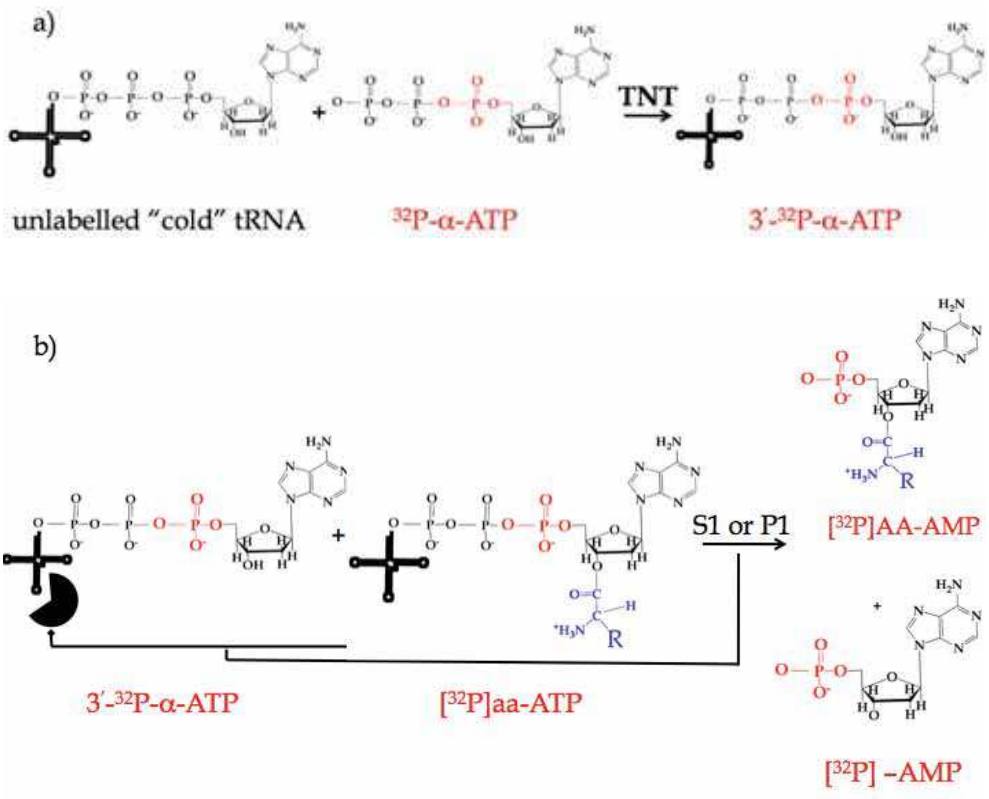

Fig. 8. Panel a) Schematic of the 3'-^{32}P labelling procedure using the repair/ processing enzyme terminal nucleotidyl transferase (TNT). Panel b) displays the hydrolysis products following enzymatic digestion with either nuclease S1 or P1.

The versatility of this assay can also be extended to monitor the aminoacylation of unnatural amino acids. We have used this assay to successfully aminoacylate a variety of natural and unnatural amino acids. As shown in Figure 9, $tRNA^{Val}$ is aminoacylated with L-Val and two unnatural amino acids: *N*-methyl val and α-hydroxy valine. The level of aminoacylation of each residue is shown in the accompanying bar graph. Figure 9b clearly shows that ValRS efficiently acylates both L- and *N*-methyl val, while α-hydroxy val is largely non-acylated. Although more detailed analysis is required to determine the exact mechanism(s) of discrimination, one can surmise that the reduced level of acylation of α-hydroxy valine is the result of the editing domain of ValRS that works in concert with $tRNA^{Val}$ to hydrolyze the α-hydroxy residue.

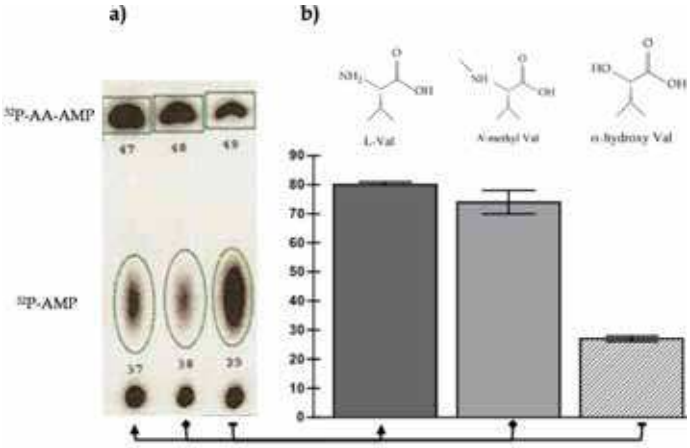

Fig. 9. Panel (a) displays the TLC image from a typical aminoacylation reaction of $tRNA^{Val}$ with three different amino acids: L-Val, *N*-methyl val and α-hydroxy valine with ValRS*. Panel (b) bar graph representation of the level of aminoacylation of each amino acid. *The concentration of ValRS (0.5 uM) was optimized/ reduced to ensure the level(s) of aminoacylation of *N*-methyl val and α-hydroxy valine were not contaminated with L-Val. Bell et al. unpublished results.

3.3 Development of a novel aminoacylation assay using ^{32}P labelled amino acids

We are currently developing a novel assay to measure the level of aminoacylation that merges the basic principles of the assays described sections in 3.1 and 3.2.2. In our assay, ^{32}P labelled amino acids are used as substrates. ^{32}P labelled amino acids are prepared using a modified version of the assay developed in the Perona laboratory (Gruic-Sovulj et al., 2005). Amino acids are radiolabelled, by incubating the substrate in the presence of ^{32}P-α-ATP and an AARS. The newly formed ^{32}P-labelled amino acid serves as a substrate for aminoacylation. This process is shown in Figure 10b. Aminoacylation is again initiated by introducing tRNA and the reaction proceeds to yield two species: acylated tRNA (aa-tRNA) and AMP. ^{32}P is highlighted in each step and serves as the readout to measure the level or rate of aminoacylation.

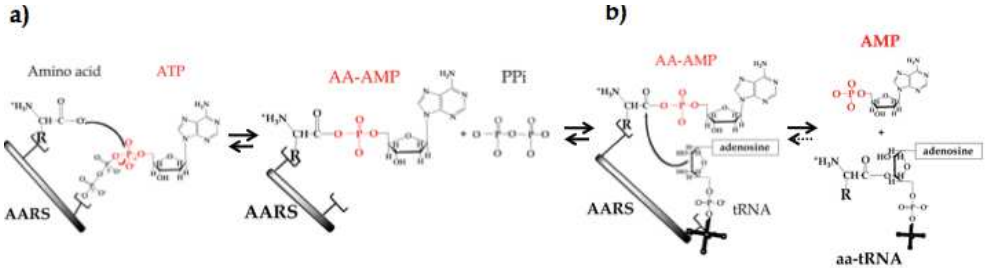

Fig. 10. Panel a) schematic displaying the formation of the ^{32}P radiolabelled amino acid [^{32}P]AA-AMP during activation. Panel b) schematic of the formation of ^{32}P-α-ATP during aminoacylation.

The readout for aminoacylation is based upon the "release" of ^{32}P-α-AMP from the activated substrate ([^{32}P]AA-AMP) as the 2′ OH of the tRNA attacks the carbonyl group of the activated amino acid. The level of aminoacylation corresponds with the increase in ^{32}P-α-AMP counts and a decrease in [^{32}P]AA-AMP counts. Each reaction component can be separated and quantified via TLC and Phoshorimager analysis. An idealized schematic displaying the electrophoretic mobility of an activated amino acid is shown in Figure 11. The radiolabelled activated (adenylate) species is denoted with the grey arrow, note there is also a measurable amount of AMP present due to spontaneous (albeit lower) hydrolysis of the activated species. The intensity (or number of counts) of the [^{32}P]AA-AMP correlates to the relative amount of activated substrate that can undergo aminoacylation.

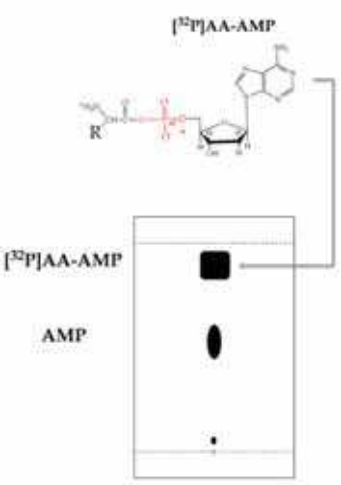

Fig. 11. Schematic of the separation of an activated amino acid generated by incubating an amino acid of interest with its cognate AARS.

In order to initiate the aminoacylation reaction, tRNAs are added in increasing amounts. The level of aminoacylation generates a measurable readout when the amounts of tRNA, AARS and amino acid approach equivalence. At this point, the level of [^{32}P]AA-AMP decreases while ^{32}P-α-AMP increases (as the radiolabelled monophosphate is released). Figure 12 displays a schematic of the change in counts of each species during a typical aminoacylation reaction.

We have used this assay to measure the aminoacylation of $tRNA^{Tyr}$ as shown in Figure 13. Eight identical reactions (containing 10 μM L-Tyr and 10 μM TyrRS) were prepared without tRNA to ensure an appreciable amount of amino acid was activated. Next, eight different amounts of tRNA was added to each tube and the reaction was incubated for 5 min. As shown in the bar graph the level of aminoacylation (^{32}P-AMP) remains relatively constant until the tRNA concentration increases to 0.50 μM (position 6, Figure 13). At this point, the ^{32}P-AMP counts begin to increase significantly. Aminoacylation is complete at tRNA levels ≥ 5 μM (position 8, Figure 13). Under these conditions, the highest amount of ^{32}P-AMP was released as noted by the large increase in ^{32}P-α-AMP counts. Conversely, the level of activated amino acid is completely consumed.

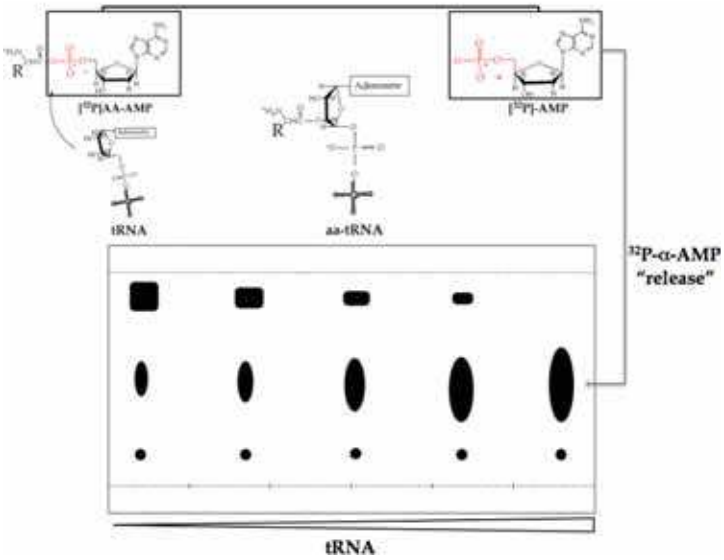

Fig. 12. Schematic illustrating separation of each radiolabelled species during a typical aminoacylation reaction containing a [32P]AA-AMP substrate. As the amount of tRNA increases the level of aminoacylation increases, this corresponds to the release (and increase in the counts) of 32P–α-AMP.

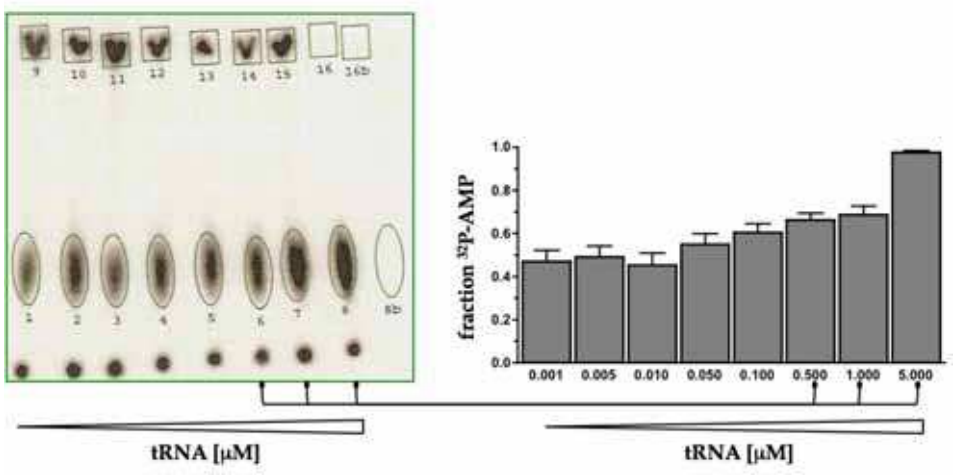

Fig. 13. Aminoacylation of 10uM activated L-Tyr with increasing amounts of $tRNA^{Tyr}$. Reaction conditions: 10.0 μM aaRS, 10 μM AA incubated at 37° C for 2 minutes to permit activation. tRNAs added to separate reaction activation reactions at concentration range of 0.001 – 5.0 μM. Each reaction quenched at 5 min in 0.1 U/ μL Nuclease P1. Reaction buffer composition: 30 mM HEPES (pH 7.0), 15 mM $MgCl_2$, 250 mM KCl, 20 mM β-mercaptoethanol, 2 μM ATP, Inorganic pyrophosphatase (0.2 U/ μL) and 32P α-ATP.

This reaction format has a number of advantages. Like the ^{32}P tRNA assay, the sensitivity of the ^{32}P signal should permit the alteration of reaction components to more closely resemble *in vivo* conditions. The assay provides a straightforward and rapid technique to measure acylation that does not require labelling of tRNAs. As a result, this assay could be used to rapidly evaluate the selectivity of tRNAs with various AARS/ AA pairs. In that, tRNAs can be rapidly screened with noncognate [^{32}P]AA-AMP substrates to determine any potential selectivity embedded within tRNAs toward noncognate amino acids. We have also used this assay to aminoacylate *in vitro* transcribed tRNAs as well (data not shown). Finally, the aminoacylation of unnatural amino acids can also be monitored. We have evaluated several unnatural amino acids (i.e. 3-fluoro tyr, 3-NO_2 tyr etc.) using this assay and each analogue displayed a similar aminoacylation trend as shown in Figure 13 (data not shown). At this stage, this assay is being used in our laboratory primarily as a qualitative tool to monitor the level of aminoacylation but we believe that it offers a tremendous level of potential to help elucidate the role of tRNAs in aminoacylation.

4. Importance of *in vitro* aa-tRNA: EF-Tu binding assays

As stated earlier, the third step in the protein synthesis pathway is the transport of aa-tRNAs to the ribosome by the bacterial translation factor EF-Tu. The process begins immediately after aminoacylation as EF-Tu binds aa-tRNAs to form a stable aa-tRNA:EF-Tu•GTP ternary complex. X-Ray crystallography data reveals that EF-Tu binds the acceptor stem and t-arm of each aa-tRNA (Figure 2) (Nissen et al., 1995; Nissen et al., 1999) to effectively "protect" the aminoacyl bond during translation. At this stage, translational fidelity is largely mediated by EF-Tu. Uhlenbeck et al. have used RNase protection assays to elegantly show that EF-Tu binds cognate aa-tRNAs within a narrow binding range (LaRiviere et al., 2001; Pleiss & Uhlenbeck, 2001; Dale et al., 2004; Ashara & Uhlenbeck, 2005; Sanderson & Uhlenbeck 2007). Their data shows that EF-Tu binds cognate aa-tRNAs with dissociation constant (K_D) values that range from 5 – 50 nM (Dale & Uhlenbeck; 2005). It is presumed EF-Tu binds cognate aa-tRNAs with near uniformity to deliver these substrates to the ribosome to undergo translation whereas misacylated or non-cognate aa-tRNAs are removed from the translational pathway. The narrow binding profile that EF-Tu has towards a limited, yet diverse set of substrates presents an interesting scenario that can be best described from an evolutionary standpoint. Uhlenbeck and others postulate that individual tRNAs and their respective cognate amino acid have co-evolved. As a result, each aa-tRNA has undergone evolutionary fine-tuning and EF-Tu binds each cognate aa-tRNA with near uniformity to mediate the next step of translation. The exact mechanism(s) that EF-Tu uses to eliminate misaclyated aa-tRNAs are unclear. Two plausible outcomes are: *i)* EF-Tu binds misacylated aa-tRNAs with a very low affinity ($K_D >> 50$ nM) and as a result AARSs may intervene to hydrolyze/ remove the misaclyated amino acid or *ii)* EF-Tu binds the misacylated aa-tRNA with an extremely high affinity ($K_D << 5$ nM) that prevents proper loading of the aa-tRNA onto the ribosome. There is also growing evidence that shows EF-Tu works in concert with the ribosome during the "initial binding" phase to ensure cognate aa-tRNAs are translated. The focus of this chapter, however, will describe the individual binding interactions between aa-tRNAs and EF-Tu.

4.1 Current *in vitro* based assays aa-tRNA: EF-Tu binding assays

RNase protection assays are one of the most prevalent techniques used to measure EF-Tu:aa-tRNA dissociation constants. The assay uses a nitrocellulose membrane to isolate aa-tRNA:EF-Tu ternary complexes that remain intact following hydrolysis with the ribonuclease, RNase A. RNase A is an ideal choice to investigate these binding interactions because the enzyme cleaves single stranded RNAs at the 3' cytosine (and uridine) position. RNase A and EF-Tu essentially compete for the same position on the aa-tRNA, with the former attempting to degrade the tRNA and latter protecting it.

To start the analysis, aa-tRNAs are generated using standard aminoacylation procedures described in sections 3.1 and 3.2.2. Next, the labelled aa-tRNAs (^{3}H, ^{14}C or ^{32}P) are purified to remove the AARS(s). The ternary complex is formed, by incubating EF-Tu with the labelled purified aa-tRNA. The RNase protection assay is capable of measuring EF-Tu dissociation constants under either equilibrium or kinetic conditions. At equilibrium conditions, the stability of individual ternary complexes is investigated. In each case, a set amount of aa-tRNA (i.e. 10 nM) is mixed with a range of EF-Tu concentrations (0.1 – 500 nM) to form a series of ternary complexes. Each reaction is initiated with the addition of RNase A at concentration known to rapidly and completely hydrolyze aa-tRNAs in the absence of EF-Tu. Each reaction is quenched (~20s), placed onto the filter binding apparatus that contains a nitrocellulose membrane and washed five times with 5-10% (w/ v) trichloroacetic acid (TCA). This step ensures an appreciable amount of ternary complex is precipitated onto the membrane. Next, the membrane is removed, dried and exposed with a Phosphorimager screen corresponding to the radiolabel of interest (^{3}H, ^{14}C or ^{32}P). Finally, the number of counts of each reaction (denoted as fraction xx-tRNA^{Xx} in Figure 14b) is plotted *vs.* the EF-Tu concentration. The midpoint or region of 50% complex corresponds to the K_D as shown in the idealized schematic in Figure 14b.

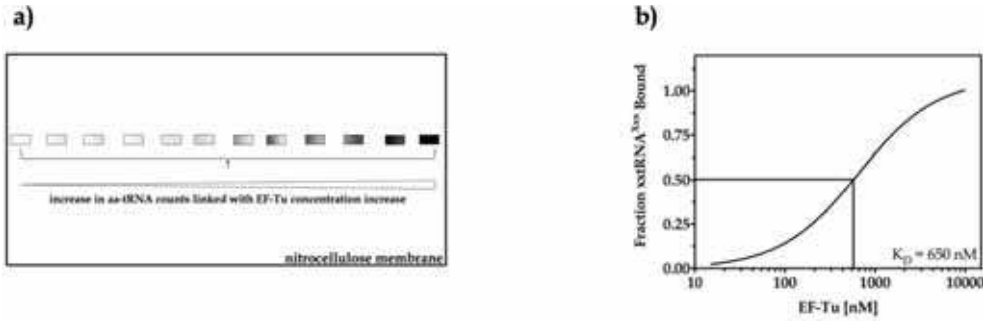

Fig. 14. Panel a) schematic of nitrocellulose membrane representing the counts remaining following the digestion of aa-tRNA:EF-Tu complex with RNase A under equilibrium conditions. Panel b) schematic of fitting analysis used to derive EF-Tu dissociation constant, K_D.

As stated earlier, the RNase protection assay can be used to measure the kinetic properties of EF-Tu binding also. In this case, the K_D is determined by calculating the rate of hydrolysis (k_{off}) of a single ternary complex. Using this format, a single ternary complex is formed by incubating an aa-tRNA (10 nM) with excess EF-Tu (100 or 1 x 10^3 nM) at 4°C for 30 minutes. Next, RNase A is added to initiate the hydrolysis reaction. During the reaction, aliquots are

removed from the reaction vessel and quenched at different time points. Each aliquot is loaded onto the filter binding apparatus and washed with TCA as described previously. Next, the counts of each aliquot are measured and the k_{off} is obtained by linear regression analysis. More specifically, the ln of counts at each time point is plotted *vs.* time (of quenching). The negative slope is equivalent to the k_{off}. Finally, the K_D is obtained by dividing the k_{off} by the on-rate constant (k_{on}). The k_{on} for typical aa-tRNA:EF-Tu complexes have been calculated as 10^5 or 10^6 $M^{-1}min^{-1}$ (LaRiviere et al., 2001).

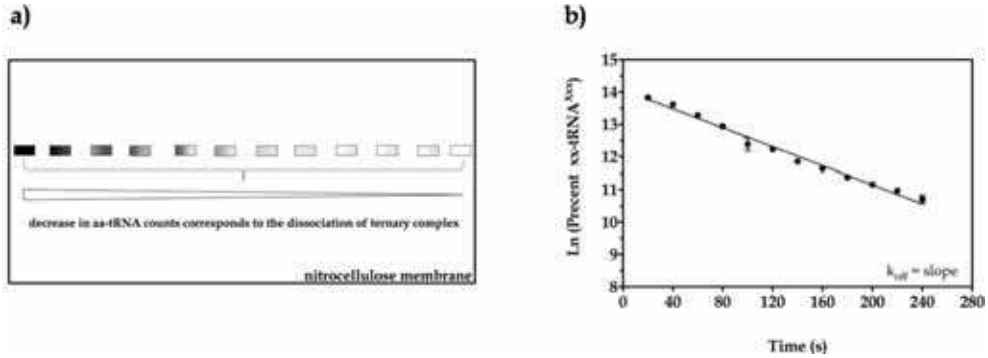

Fig. 15. Panel a) schematic of nitrocellulose membrane representing the counts remaining following the digestion of aa-tRNA:EF-Tu complex with RNase A under kinetic conditions. Panel b) schematic of linear regression analysis used to derive the off-rate constant, k_{off}.

To date, RNase protection assays could arguably be regarded as the gold standard for measuring EF-Tu binding constants. These assays have proven to be a workhouse technique that has provided an enormous level of insight toward to underlying mechanisms of translation. However, there are significant disadvantages associated with protection assays. The primary drawback is the large amount of experimental variability associated with these assays. Reports show that these assays can typically generate between 20 to 40% variability per analysis. The high level of variance may be related to the weak signal strength associated with the ^3H and ^{14}C, while ^{32}P despite being more sensitive again requires shielding for protection. These reasons show that despite its success there is a need to develop additional assays to investigate the binding properties of EF-Tu to aa-tRNAs.

4.2 Development a novel fluorescent assay to monitor aa-tRNA: EF-Tu binding interactions

We are currently developing a fluorescence based polyacrylamide gel assay as an alternate technique to measure EF-Tu:aa-tRNA binding interactions. A fluorescence-based assay was selected because this method offers a reliable and safe method to measure EF-Tu binding that would circumvent the drawbacks related to the variability and safety of ^{14}C and ^{32}P assays. The assay follows a similar procedure to those described in section 4.1 with three noted exceptions: *i)* a fluorophore is conjugated to the tRNA prior to aminoacylation, *ii)* an RNase mixture (RNase A/ T1, Ambion) is used to hydrolyze aa-tRNAs and *iii)* a native PAGE gel is used to separate hydrolyzed aa-tRNAs from the in tact ternary complexes.

4.2.1 Conjugation of tRNA with fluorescent label

For our analysis the thiol-reactive Alexa Fluor® 488 C_5 maleimide dye was selected to label the tRNA. The maleimide functional group provides an ideal molecular handle that can undergo a coupling reaction with the thiouridine (s4U) tRNA hyper-modified base. The reaction is non-enzymatic and proceeds to completion in 2 hours at 37°C or in 12-16 hours at 4°C. The labelled tRNA is separated from non-conjugated dye via phenol/ chloroform/ isoamyl extraction or NAP column purification. Figure 16a displays the structures of Alexa Fluor 488 C_5 maleimide and s4U. The location of s4U within the single stranded region connecting the D-arm and acceptor stem is displayed in Figure 16b.

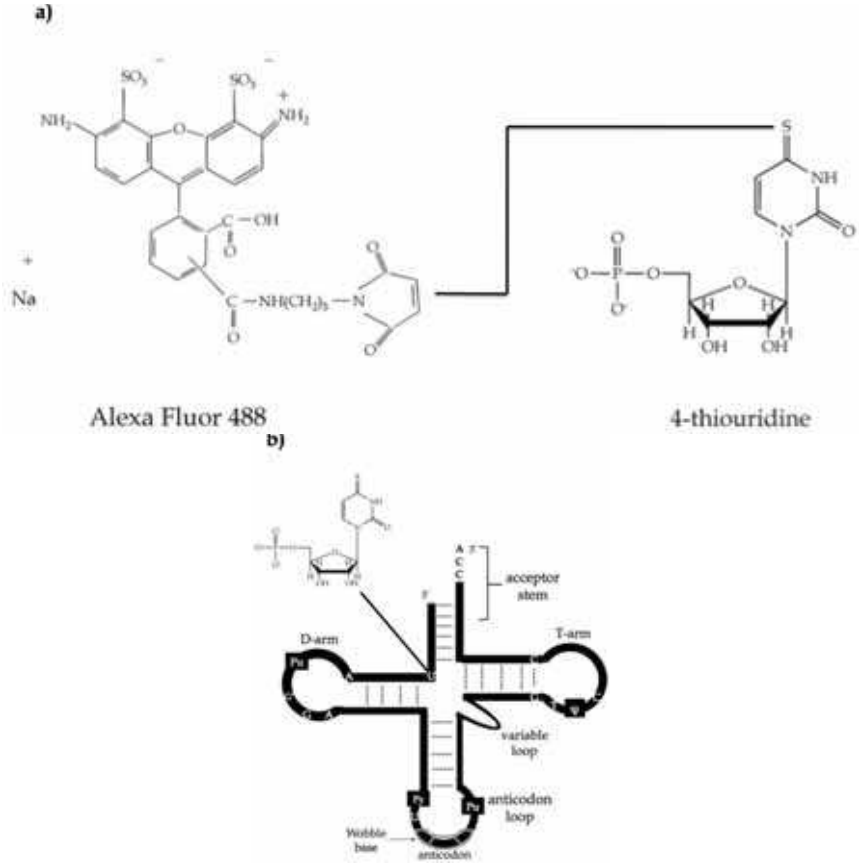

Fig. 16. Panel a) schematic of Alexa Fluor 488 maleimide and 4-thiouridine functional groups. Panel b) location of the 4-thiouridine hyper-modified base within the secondary structure of tRNA.

4.2.2 Aminoacylation characteristics of fluorescently labelled aa-tRNAs

Despite the advantages related to safety and ease of conjugation, the presence of a relatively large fluorophore near the tRNA acceptor stem could potentially perturb the aminoacylation. To address this issue, we have measured the aminoacylation of tRNAs

labelled with both ^{32}P and Alexa Fluor 488. Figure 17 displays a TLC image of the aminoacylation profile of $tRNA^{Tyr}$ with L-Tyr and series of unnatural amino acids. As evidenced in the high levels of acylation (> 70%) for L-Tyr (position 1) and 3-fluoro tyr (position 3), the presence of the dye does not have a deleterious effect on aminoacylation. The reduced level of acylation for the remaining unnatural amino acids (positions 2, 4 and 5) is consistent with data using tRNAs labelled solely with ^{32}P (data not shown). Hence, the reduced aminoacylation levels for these samples are presumably the result of editing by TyrRS and not the fluorophore.

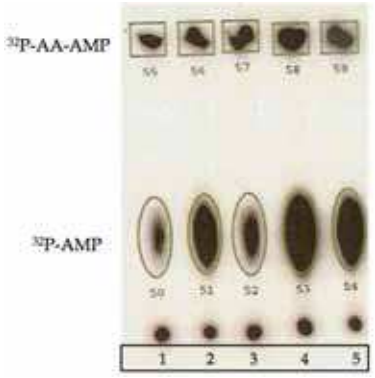

Fig. 17. Aminoacylation of dual labelled $tRNA^{Tyr}$. The tRNA is labelled with ^{32}P and Alexa Fluor 488. The level of aminoacylation is recorded based on the technique discussed in section 3.2.2. The resulting aa-tRNAs correspond to $tRNA^{Tyr}$ acylated with the following amino acids in lanes 1 – 5: L-Tyr(lane 1), 3-nitro tyr (lane2), 3-fluouro tyr (lane 3), *N*-methyl tyr (lane 4) and α-hydroxy tyr (lane 5).

4.2.3 Hydrolysis of fluorescently labelled aa-tRNAs

The positioning/ conjugation of the fluorophore to a uridine base within a single stranded region of the tRNA is a critical feature of the assay. As stated earlier, RNase A hydrolyzes substrates at cytosine and uridine residues. Therefore, the fluorescent aa-tRNA should be hydrolyzed in a similar fashion as described in section 4.1. To ensure the aa-tRNA undergoes complete hydrolysis, we employed an RNase enzyme mixture composed of the RNases A and T1. RNase T1 is an exonuclease that cleaves at single stranded guanine residues. We presume that RNase A will provide the driving force to initiate hydrolysis due to its relatively higher activity than RNase T1. A comparison of the hydrolytic activity of the RNase A/ T1 mixture *vs.* RNase III and RNase VI reveal that RNase A/ T1 is the most effective (data not shown). Figure 18 displays the hydrolysis of the fluorescent $ValtRNA^{Val\text{-}488}$, in the presence of RNase A/ T1. Lane 1 corresponds to the intact aa-tRNA in the absence of the RNase cocktail. Lanes 2 – 8 correspond to $ValtRNA^{Val\text{-}488}$ hydrolyzed with RNase A/ T1 at time points of 5, 10, 15, 20, 25, 30 and 60 seconds. As noted in lanes 2-8, intact $ValtRNA^{Val\text{-}488}$ is rapidly hydrolyzed. The major hydrolyzed species is presumably a longer segment(s) of the labelled 5'end; while the faster running species correspond to a heterogeneous mixture of hydrolyzed labelled tRNAs.

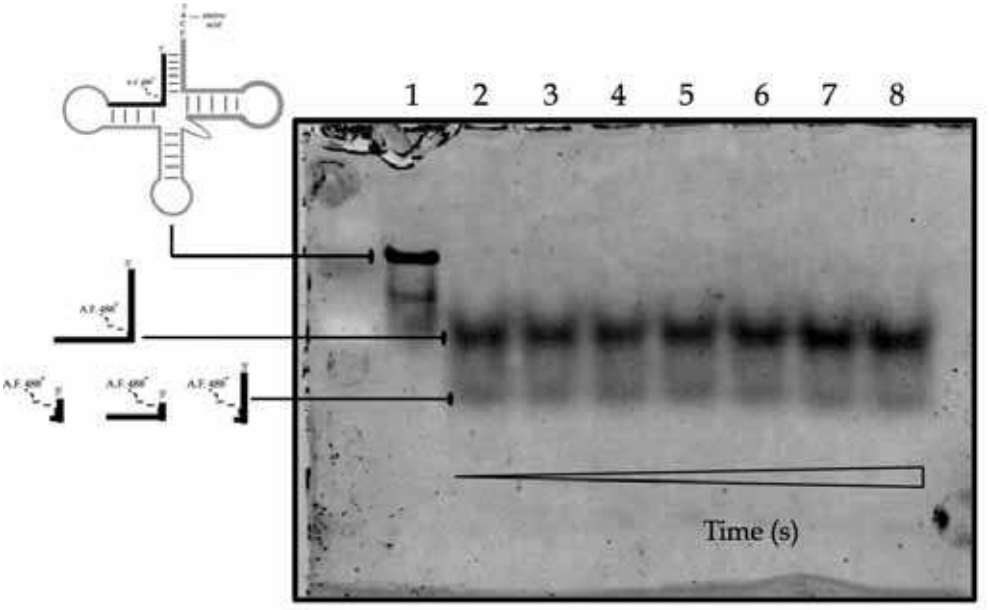

Fig. 18. Polyacrylamide gel analysis of the hydrolysis of labelled ValtRNA$^{Val\text{-}488}$ with the RNase cocktail – RNase A/ T1. Lane 1 corresponds to 5.0μM ValtRNA$^{Val\text{-}488}$ in the absence of RNases. Lanes 2 – 8 correspond to individual ValtRNA$^{Val\text{-}488}$ (5.0μM) samples incubated with RNase A/ T1 cocktail (1.25 Units A & 50 Units T1) for 5, 10, 15, 20, 25, 30 and 60 seconds, respectively. Each reaction was quenched with unfractionated yeast total tRNA (1.0 mg/ mL). Gel conditions: 15% tris boric acid gel, 1X TBE running buffer (90 mM Trisma, 90 mM boric acid and 2 mM EDTA), run time 4 hours at 4^{o}C.

4.2.4 Evaluation of EF-Tu binding properties to fluorescent aa-tRNAs

This assay like the filter binding assay described in section 4.1 can be utilized to measure aa-tRNA:EF-Tu binding constants under equilibrium and kinetic conditions. Thus far we have only investigated the kinetic reaction format. One critical feature that must be determined is the optimum RNase concentration that will permit reliable off rate measurements. The RNase concentration used in Figure 18 (1.25 Units RNase A & 50 Units RNase T1) degrades the ternary complex too rapidly to reliable measure the kinetics. To address, a series of lower RNase concentrations have been used to measure stability of EF-Tu:aa-tRNA ternary complexes. Figure 19 shows the typical hydrolysis profile of ValtRNA$^{Val\text{-}488}$ bound to EF-Tu. Panel a) displays the hydrolysis profile of the ternary complex using an RNase cocktail concentration composed of 5 x 10^{-4} and 0.02 units of RNAase A and T1. Panel b) displays the hydrolysis profile of the ternary complex using lower amounts of RNases. In this case, 1 x 10^{-4} and 4 x 10^{-3} units of RNase A and T1 are employed. As shown below, the second RNase concentration is more amenable to measuring EF-Tu binding characteristics since the complex is present throughout the duration of the reaction (2 – 120 seconds).

Using these RNase concentrations as a baseline, the reaction was extended to longer time points in order to obtain k_{off} measurements. As shown in Figure 20 lanes 5 – 9, the complex degrades gradually in the presence of the RNase cocktail. The diminished level of ternary

complexes (lanes 5-7) corresponds with an increase in the level of hydrolyzed products. The accompanying graph displays the hydrolysis profile of the reaction. Although this data is unable to be fit via linear regression analysis, it does indicate the ternary complex dissociates appreciably with time.

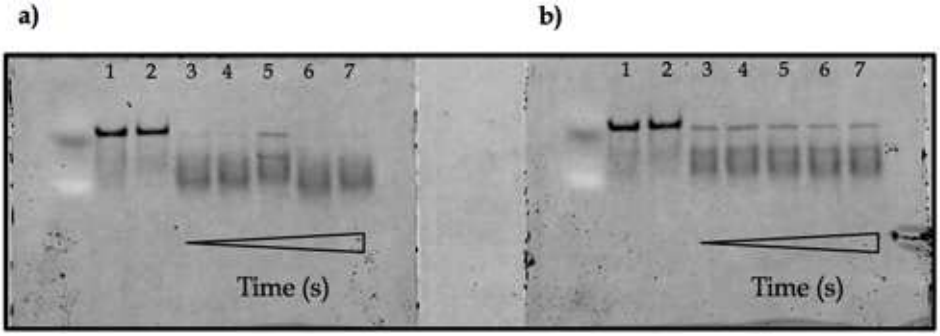

Fig. 19. Polyacrylamide gel analysis of the hydrolysis of ValtRNA$^{Val\text{-}488}$:EF-Tu ternary complex with RNase A/ T1 cocktail. Ternary complex composed of ValtRNA$^{Val\text{-}488}$ (0.5 μM) and EF-Tu (5.0 μM). Panel a) RNase A/ T1 cocktail (5 x 10^{-4} Units A & 0.02 Units T1), panel b) RNase A/ T1 cocktail (1 x 10^{-4} Units A & 4.0 x 10^{-3} Units T1). Lane 1 ValtRNA$^{Val\text{-}488}$ (0.5 μM), lane 2 ValtRNA$^{Val\text{-}488}$:EF-Tu (0.5 μM and 5.0 μM), lanes 3 – 7 corresponds to reaction run times of 2, 5, 10, 30 and 120 seconds, respectively. Each reaction was quenched with unfractionated yeast total tRNA (1.0 mg/ mL). Gel conditions: 15% tris boric acid gel, 1X TBE running buffer (90 mM Trisma, 90 mM boric acid and 2 mM EDTA), run time 4 hours at 4°C.

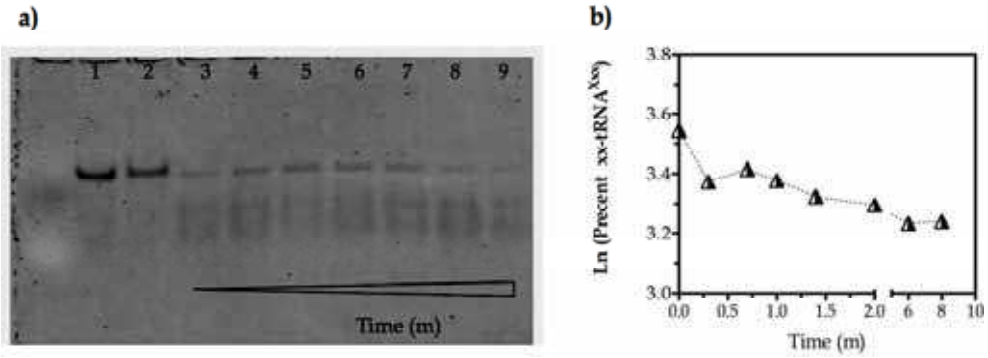

Fig. 20. Polyacrylamide gel analysis of the hydrolysis of ValtRNA$^{Val\text{-}488}$:EF-Tu ternary complex with RNase A/ T1 cocktail. Ternary complex composed of ValtRNA$^{Val\text{-}488}$ (0.5 μM) and EF-Tu (5.0 μM), RNase A/ T1 cocktail (1 x 10^{-4} Units A & 4.0 x 10^{-3} Units T1). Lane 1 ValtRNA$^{Val\text{-}488}$ (0.5 μM), lane 2 ValtRNA$^{Val\text{-}488}$:EF-Tu (0.5 μM and 5.0 μM), lanes 3 – 9 corresponds to reaction run times of 0.3, 0.7, 1, 1.4, 2, 6 and 8 minutes, respectively. Each reaction was quenched with unfractionated yeast total tRNA (1.0 mg/ mL). Gel conditions: 15% tris boric acid gel, 1X TBE running buffer (90 mM Trisma, 90 mM boric acid and 2 mM EDTA), run time 4 hours at 4°C.

The hydrolysis profile is very inconsistent at time points < 40 sec (Figure 20 and additional data not shown). One possible approach to improve the hydrolysis profile may be related to the optimization of the RNase composition. The inconsistent hydrolysis profile may occur

since three enzymes are effectively competing for a single aa-tRNA. RNAse T1 is present at nearly 50-fold excess to RNase A but despite the large excess of RNase T1 this enzyme is much less reactive. As a result, RNase T1 may actually inhibit or reduce the efficacy of RNase A at the initial stage(s) of the reaction. We are currently investigating the hydrolysis of ternary complexes using RNase A alone.

5. Conclusion

We have presented two new assays that we believe can be used to further elucidate the role of tRNA in aminoacylation and aa-tRNA transport. The aminoacylation assay merges concepts from established techniques, while offering a novel approach to measure aminoacylation. The new assay does not require labelling of tRNAs. Therefore, the aminoacylation procedure is more straightforward. The presence of the ^{32}P radioisotope provides an extremely sensitive signal. Therefore, the reaction conditions can be readily changed – this feature enables the investigation of aminoacylation under standard *in vitro* and *in vivo*-like conditions. The second assay uses fluorescently labelled aa-tRNAs as substrates to monitor the stability of aa-tRNA:EF-Tu ternary complexes. The assay is unique in that it uses a fluorophore that is site specifically conjugated to a single-stranded region of the tRNA. The location of the fluorophore within this region is critical for two reasons: *i)* labels (moieties) located at the 5' or 3' terminus could deleteriously affect aminoacylation and *ii)* standard RNases (i.e. RNase A) should generate a predictable hydrolysis profile. Despite the ease of use of this system the fluorophore does not supply the same sensitivity as provided by ^{32}P. However, the lack of sensitivity may be offset by the fact that the "entire" reaction volume can be loaded onto a gel and subsequently quantified.

6. References

Asahara, H. & Uhlenbeck, O.C. (2005) Predicting the binding affinities of miscacylated tRNAs for Thermus thermophilus EF-Tu.GTP, *Biochemistry*, Vol. 23 No. 44 pp. 11254-11261.

Beuning, P.J, Yang, F., Schimmel, P. & Musier-Forsyth, K. (1997) Specific atomic groups and RNA helix geometry in acceptor stem recognition by a tRNA synthetase, *Proc Natl Acad Sci U. S. A.*, Vol. 16 No. 19 pp. 10150-10154.

Crick, F.H. (1958) On protein synthesis, *Symp. Soc. Exp. Biol.*, Vol. 12 pp. 138-163.

Dale, T., Sanderson, L.E. & Uhlenbeck, O.C. (2004) The affinity of elongation factor Tu for an aminoacyl-tRNA is modulated by the esterified amino acid, *Biochemistry*, Vol. 43 No. 20 pp. 6159-6166.

Dale, T. & Uhlenbeck, O.C. (2005) Amino acid specificity in translation, *Trends Biochem Sci.*, Vol. 30 No. 12 pp. 659-665.

Deutscher, M.P. (1982) tRNA nucleotidyl transferase, *The Enzymes*, Vol. 15 pp. 183-215.

Dunin-Horkawicz, S., Czerwoniec, A., Gajda, M.J, Feder, M., Grosjean, H. & Bujnicki, JM. (2006) MODOMICS: a database of RNA modification pathways, *Nucleic Acids Res.*, Vol. 34 (Database issue) D145-149.

Eigner, E.A. & Loftfield, R.B. (1974) Kinetic techniques for the investigation of amino acid: tRNA ligases (aminoacyl-tRNA synthetases, amino acid activating enzymes), *Methods Enzymol.*, Vol. 29 pp. 601-619.

Eriani, G., Cavarelli, J., Martin, F., Dirheimer, G., Moras, D. & Gangloff, J. (1993) Role of dimerization in yeast aspartyl-tRNA synthetase and importance of the class II invariant proline, *Proc Natl Acad Sci U.S.A.*, Vol. 90 No. 22 pp. 10816-108120.

Francklyn, C. & Schimmel, P. (1989) Aminoacylation of RNA minihelices with alanine, *Nature*, Vol. 337 No. 6206 pp. 478-481.

Frank, D.N. & Pace, N.R. (1998) Ribonuclease P: unity and diversity in a tRNA processing ribozyme, *Annu. Rev. Biochem.*, Vol. 67 pp.153-180.

Gabriel, K., Schneider, J. & McClain, W.H. (1996) Functional evidence for indirect recognition of G.U in tRNA(Ala) by alanyl-tRNA synthetase, *Science*, Vol. 271 No. 5246 pp. 195-197.

Giegé, R., Sissler, M., & Florentz C. (1998) Universal rules and idiosyncratic features in tRNA identity, *Nucleic Acids Res.* Vol. 15 No. 26, pp. 5017-5035.

Gruic-Sovulj, I., Uter, N., Bullock, T. & Perona, J.J. (2005) tRNA-dependent amionayl-adenylate hydrolysis by a nonediting class I aminoacyl-tRNA synthetase, *JBiol Chem.*, Vol. 280 pp. 23978-23986.

Hill, K. & Schimmel, P. (1989) Evidence that the 3' end of a tRNA binds to a site in the adenylate synthesis domain of an aminoacyl-tRNA synthetase, *Biochemistry*, Vol 28 No. 6 pp. 2577-2586.

Hoagland, M.B., Zamecnik, P.C. & Stephenson, M.L., (1957) Intermediate reactions in protein biosynthesis, *Biochim Biophys Acta*, Vol. 24 pp. 215-216.

Holley, R.W., Everett, G.A., Madison, J.T. & Zamir, A. (1965) Nucleotide sequences in the yeast alanine transfer nucleic acid, *JBiol Chem.* Vol. 240 pp. 2122-2128.

Hou, Y.M. & Schimmel, P. (1988) A simple structural feature is a major determinant of the identity of a transfer RNA, *Nature*, Vol. 333 No. 6169 pp. 140-145.

Hussain, T., Kruparani, S.P., Pal, B., Dock-Bregeon, A.C., Dwivedi, S., Shekar, M.R., Sureshbabu, K. & Sankaranarayanan, R. (2006). Post-transfer editing mechanism of a D- aminoacyl-tRNA deacylase-like domain in threonyl-tRNA synthetase from archaea, *EMBO Journal*, Vol. 25 No. 17, pp. 4152-4162.

Ibba, M., Hong, K.W., Sherman, J.M., Sever, S. & Söll, D. (1996) Interactions between tRNA identity nucleotides and their recognition sites in glutaminyl-tRNA synthetase, determine the cognate amino acid affinity of the enzyme, *Proc Natl Acad Sci U.S.A.*, Vol. 93 No. 14 pp. 6953-6958.

Iwata-Reuyl, D. (2008) An embarrassment of riches: the enzymology of RNA modification, *Curr Opin Chem Biol.* Vol. 12 No. 2 pp. 126-133.

LaRiviere,. F.J, Wolfson, A.D. & Uhlenbeck, O.C. (2001) Uniform binding of aminoacyl-tRNAs to elongation factor Tu by thermodynamic compensation, *Science*, Vol. 294 No. 5540 pp. 165-168.

Ling, J, Reynolds, N. & Ibba M. (2009) Aminoacyl-tRNA synthesis and translational quality control, *Annu Rev Microbiol.*, Vol. 63 pp. 61-78.

Loftield, R.B. & Vanderjagt, D. (1972) The frequency of errors in protein biosynthesis, *Biochem J*, Vol. 128 No. 5, pp. 1353-1356.

Loftfield, R.B. (1972) The mechanism of aminoacylation of transfer RNA, *Prog Nucleic Acid Res Mol Biol.*, Vol. 12 pp. 87-128.

Martin, N.C., Rabinowitz, M. & Fukuhara, H. (1977) Yeast mitochondrial DNA specifies tRNA for 19 amino acids. Deletion mapping of the tRNA genes, *Biochemistry*, Vol. 16 No. 21 pp. 4672-4677.

McClain, W.H., Chen, Y.M., Foss, K. & Schneider, J. (1988) Association of transfer RNA acceptor identity with a helical irregularity, *Science*, Vol. 242 No. 4886 pp. 1681-1684.

McClain, W.H., Jou, Y.Y., Bhattacharya, S., Gabriel K, Schneider J. (1999) The reliability of in vivo structure-function analysis of tRNA aminoacylation, *JMol Biol.*, Vol. 290 No. 2pp. 391-409.

Morl, M. & Marchfelder, A. (2001) The final cut. The importance of tRNA 3'-processing, *EMBO reports*, Vol. 2 No. 1 pp. 17-20.

Musier-Forsyth, K., Usman, N., Scaringe, S., Doudna, J., Green, R., & Schimmel P. (1991) Specificity for aminoacylation of an RNA helix: an unpaired, exocyclic amino group in the minor groove, *Science*, Vol. 253 No. 5021 pp. 784-786.

Nissen, P., Kjeldgaard, M., Thirup, S., Polkenhina, S., Reshetnikova, L., Clark, B.F. & Nyborg J. (1995) Crystal structure of the ternary complex of Phe-tRNAPhe, EF-Tu, and a GTP analog, *Science*, Vol. 270 pp.1464-1472.

Nissen, P., Thirup, S., Kjeldgaard, M. & Nyborg J. (1999) The crystal structure of Cys-tRNACys-EF-TuGDNP reveals general and specific features in the ternary complex and in tRNA, *Structure Fold. Des*, Vol. 7 pp. 143-156.

Ogle, JM. & Ramakrishnan, V. (2005) Structural insights into translational fidelity, *Annu Rev Biochem.*, Vol. 74 pp. 129-177.

Pleiss, JA. & Uhlenbeck, O.C. (2001) Identification of thermodynamically relevant interactions between EF-Tu and backbone elements of tRNA, *JMol Biol.*, Vol. 308 No. 5 pp. 895-905.

Sanderson, L.E. & Uhlenbeck, O.C. (2007) Exploring the specificity of bacterial elongation factor Tu for different tRNAs, *Biochemistry*, Vol. 46 No. 21 pp. 6194-6200.

Reynolds, N.M., Lazazzera, B.A. & Ibba, M. (2010) Cellular mechanisms that control mistranslation, *Nat Rev Microbiol.*, Vol. 8 pp. 849-856.

Rosenberger, R.F. & Foskett, G. (1981) An estimate of the frequency of in vivo transcriptional errors at a nonsense codon in Escherichia coli, *Mol Gen Gent,* Vol. 183 No. 3, pp. 561-563.

Roy, H. & Ibba, M. (2006) Molecular biology: sticky end in protein synthesis, *Nature*, Vol. 443 No. 7107 pp. 41-42.

Rozenski, J., Crain, P.F. & McCloskey, JA. (1999) The RNA Modification Database: 1999 update, *Nucleic Acids Res.*, Vol. 27 No. 1 pp. 196-197.

Sprinzl, M. & Cramer, F. (1997) The -C-C-A end of tRNA and its role in protein biosynthesis, *Prog Nucleic Acid Res Mol Biol.,* Vol. 22 pp. 169.

Wilcox, M. & Nirenberg, M. (1968) Transfer RNA as cofactor coupling amino acid synthesis with that of protein, *Proc. Natl. Acad. Sci. U.S.A.*, Vol. 61 pp. 229-236.

White, B.N. & Bayley, S. T. (1972) Further codon assignments in an extremely halophilic bacterium using a cell-free protein-synthesizing system and a ribosomal binding assay, *Can. J Biochem.*, Vol. 50 pp. 600-609.

Wolfson, A.D., Pleiss, JA. & Uhlenbeck, O.C. (1998) A new assay for tRNA aminoacylation kinetics, *RNA*, Vol. 4 No. 8 pp. 1019-1023.

Wolfson, A.D. & Uhlenbeck, O.C. (2002) Modulation of tRNAAla identity by inorganic pyrophosphatase, *Proc Natl Acad Sci U.S.A.*, Vol. 99 No. 9 pp. 5965-5970.

Yue, D., Maizels, N. & Weiner, A.M. (1996) CCA-adding enzymes and poly(A) polymerases are all members of the same nucleotidyltransferase superfamily: characterization of the CCA-adding enzyme from the archaeal hyperthermophile Sulfolobus shibatae, *RNA,* Vol. 2 No. 9 pp. 895-908.

Zachau, H.G., Acs, G. & Lipmann F. (1958) Isolation of adenosine amino acid esters from a ribonuclease digest of soluble, liver ribonucleic acid, *Proc. Natl. Acad. Sci., U.S.A.*, Vol. 44 No. 9 pp. 885-889

Zhu, L. & Deutscher, M.P. (1987) tRNA nucleotidyltransferase is not essential for Escherichia coli viability, *EMBO J*, Vol. 6 No. 8 pp. 2473-2477.

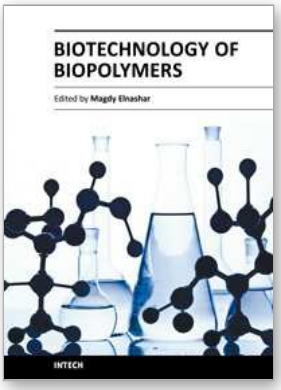

Biotechnology of Biopolymers

Edited by Prof. Magdy Elnashar

ISBN 978-953-307-179-4
Hard cover, 364 pages
Publisher InTech
Published online 24, June, 2011
Published in print edition June, 2011

The book "Biotechnology of Biopolymers" comprises 17 chapters covering occurrence, synthesis, isolation and production, properties and applications, biodegradation and modification, the relevant analysis methods to reveal the structures and properties of biopolymers and a special section on the theoretical, experimental and mathematical models of biopolymers. This book will hopefully be supportive to many scientists, physicians, pharmaceutics, engineers and other experts in a wide variety of different disciplines, in academia and in industry. It may not only support research and development but may be also suitable for teaching. Publishing of this book was achieved by choosing authors of the individual chapters for their recognized expertise and for their excellent contributions to the various fields of research.

InTech Europe
University Campus STeP Ri
Slavka Krautzeka 83/A
51000 Rijeka, Croatia
Phone: +385 (51) 770 447
Fax: +385 (51) 686 166
www.intechopen.com

InTech China
Unit 405, Office Block, Hotel Equatorial Shanghai
No.65, Yan An Road (West), Shanghai, 200040, China
中国上海市延安西路65号上海国际贵都大饭店办公楼405单元
Phone: +86-21-62489820
Fax: +86-21-62489821